Constrained Safety-Integrity Performance of Through-the-Arms UHF-RFID Transcutaneous Wireless Communication for the Control of Prostheses

Carolina Miozzi, Giovanni Saggio, Emanuele Gruppioni, and Gaetano Marrocco

***Abstract*—Advanced prostheses for recovery of arm amputation can be nowadays controlled by the electromyographic (EMG) signals. Implanted myoelectric sensors, suitable to transcutaneous wireless reading, permit to improve the signal-to-noise ratio. This paper explores the feasibility of a through-the-arm telemetry link based on the radiofrequency identification in the UHF band (860–960 MHz). The proposed model accounts for the power sensitivity of the commercial devices, the constraints enforced by the exposure regulations (SAR) and by the communication integrity (BER). The reliability of the link is evaluated against possible misalignments between sensors and the reading unit. Results demonstrate that the transcutaneous link can be in some case limited by integrity constraints but can be nevertheless correctly established by means of less than 23 dBm input power (full compatible with embedded readers). The link is moreover robust against angular displacement up to at least $\Delta\phi = \pm 35°$ and linear displacement up to 2.5 cm.**

***Index Terms*—Radiofrequency identification, robotic limb, transcutaneous wireless communication, implantable device.**

I. Introduction

STATE of the art prostheses for arm amputation recovery are controlled by the electromyographic (EMG) signals [1] generated by the electric potential difference (typically 70-90 mV peak [2]) between the outside and the inside of the muscular cells during muscle contraction. EMG signals are generally collected by surface-mounted sensors [3], [4] that have however several disadvantages since they are exposed to the variation of skin impedance due to sweat and could detach. They are moreover characterized by a low signal-to-noise ratio due to the absorption of the myoelectric signals by muscle/fat/skin layers. To overcome some of the above problems, myoelectric sensors could be implanted in the arms [1], [3] and be interrogated from the prosthesis through a transcutaneous wireless link. A pioneering system [5], [6] operating in battery-less mode comprised two coupled planar coils (diameters: 6 mm for implanted antenna and 2 cm for external unit placed into the socket) tuned at 8 MHz. Imperfect mounting and dismantling of the prosthesis (at least once per day) may in this case produce misalignment [7] between sensors and interrogator and accordingly a degradation of the link. The Implantable MyoElectric Sensor (IMES) [8], [9], [10] (diameter: 2.5 mm; length: 16 mm) resorted to a 121 kHz link. The interrogator device was in this case a large coil wrapped onto the socket that hence needs a manual customization for each patient.

This paper explores the feasibility of a different kind of wireless link involving the Radiofrequency Identification (RFID) technology in the UHF band (860-960 MHz) that is expected to offer some potential advantages such as increasingly availability of off-the-shelf sensor-oriented microchip transponders and readers and more freedom in the shaping of the interrogating antenna. This, could be attached onto the prosthesis like a thin plaster, reducing the need of manual customization. Moreover, as a UHF reader allows a much longer read range than lower-frequency ones, it could also enable the prosthesis to interact, with the external environment according to the framework of Internet of Things and Smart Spaces [11], thus providing the patient with augmented senses [12]. UHF systems have however to face within the much higher losses of the human body. The expected consequence is a stronger power absorption inside tissues so that the constraint over the maximum allowed Specific Absorption Rate (SAR) could become critical for the feasibility of the transcutaneous communication based on backscattering modulation.

Preliminary tradeoff analysis for the RFID link of implanted RFID sensors, including also SAR considerations, were reported in [13] and in [14] concerning the monitoring of vascular stents and orthopedic prostheses, respectively. But in those cases the interrogating antenna was placed up to 20-30 cm from the skin and the estimated SAR resulted greatly below the limits. The feasibility of transcutaneous UHF-RFID telemetry, with the interrogating antenna placed this time at a very close distance from the skin, was investigated in [15] concerning wireless brain-machine interfaces. SAR compliance revealed a potential limiting factor to establish the link. Nevertheless, such analysis only considered the direct link (from reader to the tag) while no result was

Manuscript received January 21, 2019; revised April 27, 2019; accepted May 20, 2019. This work was supported in part by the Istituto Italiano di Tecnologia and in part by the Istituto Nazionale Assicurazione Infortuni sul Lavoro—Centro Protesi under Contract PPR AS 1/1, Task 1.5. *(Corresponding author: Gaetano Marrocco.)*

C. Miozzi, G. Saggio, and G. Marrocco are with the University of Roma Tor Vergata, 00133 Rome, Italy (e-mail: gaetano.marrocco@uniroma2.it).

E. Gruppioni is with INAIL Centro Protesi, Research and Training Area, Budrio, Italy.

Digital Object Identifier 10.1109/JRFID.2019.2921097

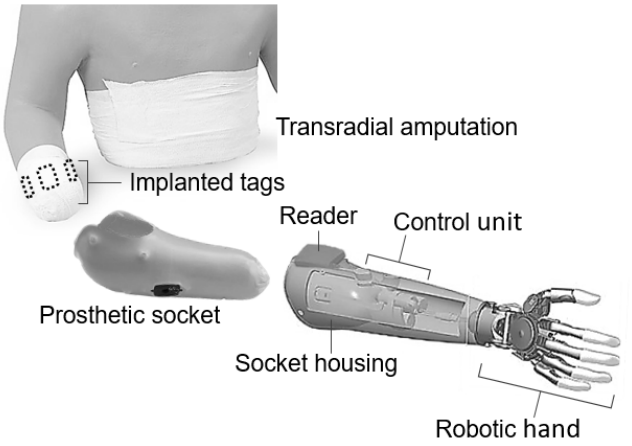

Fig. 1. Sketch of transcutaneous communication system for the control of upper-limb myoelectric prostheses.

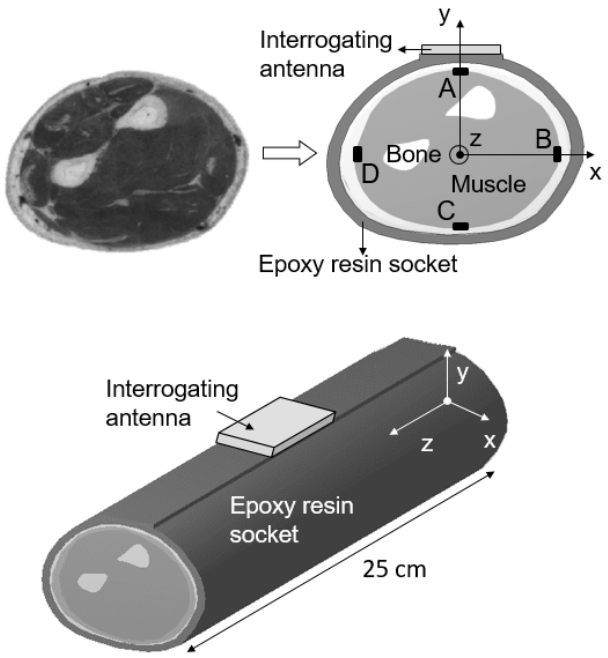

Fig. 2. Multilayered forearm and socket model with indication of the interrogation antenna and of four possible positions of the implanted loop. Length: 25 cm; cross section: 70 $mm \times 50\,mm$. Electromagnetic parameters: skin: $\varepsilon_r = 41.6$, $\sigma = 0.8\,S/m$; fat: $\varepsilon_r = 5.5$, $\sigma = 0.05\,S/m$; muscle: $\varepsilon_r = 55.1$, $\sigma = 0.9\,S/m$; bone: $\varepsilon_r = 12.5$, $\sigma = 0.1\,S/m$; epoxy resin: $\varepsilon_r = 4$, $\sigma = 6 \cdot 10^{-4}\,S/m$.

provided concerning the quality of the data-link. Overall, the state of the art does not provide enough information to assess the feasibility of an RFID-UHF transcutaneous link in real conditions accounting for all the electrical and geometrical parameters.

Starting from the above results, and from the preliminary conference paper [16] with over-simplified models, this work introduces a more detailed electromagnetic formulation (Section II) and arm representation. It exploits both the wireless power transfer link and the backscattering communication, realistic sensitivities of sensor-oriented microchip and an ad-hoc formulation of the Bit Error Rate (BER) for a two-port RFID system (Section III). The goal is to estimate through numerical analysis (Section IV) and some preliminary experimental corroboration (Section V), read volume of implanted sensors inside the arm that is compatible with all the electrical and safety parameters [17], also including possible misalignment of the sensors and the communication integrity, and to compare them with the performance of corresponding HF systems.

II. Through-the-Arm Telemetry System

A typical upper limb myoelectric prosthesis (Fig. 1) comprises an electro-mechanical device replacing the hand itself with grasp capability and a custom-made resin socket, suitable to perfectly adhere to the arm stump of the patient, where the prosthesis will be mechanically inserted.

EMG sensors generally comprise a couplet of conductive electrodes to be applied at a few millimeters distance [18] and require a 1-5 V bias voltage. The myoelectric signal detected from the electrodes is inversely proportional to the distance from the source [2], but after an internal amplification to the EMG sensor, the output signal peak is of the order of 0.5-2 V [19], depending on the gain. Typical sampling rate for the accurate signal tracing is of the order of 1 kHz [18]. However, a much coarser sampling frequency could be enough to just extract a few features of the signal to control some gestures of the hand prosthesis [20]. The exact determination of the minimum sampling rate in case of implanted sensors, when a better signal to noise ratio is expected, is processing-dependent and is currently outside the scope of this paper that is instead only focused on the radiofrequency transcutaneous link independently on the EMG sensor features ad shape.

In order to implement a wireless sampling of the myoelectric signals directly at the level of the muscular fibers of the stump, it is assumed to implant small-size RFID transponders between the fat and the muscle layers at positions {*A, B, C, D*}, where EMG sensors should be ideally located (Fig. 2). Positions *A* and *C* are hereafter considered as the reference implants to sample both the agonist and antagonist forearm muscles that are involved in the main movements of fingers and wrist. Position *B* and *D* refer to sensors implanted in the lateral fat-muscle interface w.r.t. the bone, and they are also representative of extreme cases of axial migration of implanted tags. Sensors will be powered and interrogated by means of one or more low-size and conformable antennas placed on the interface between the prosthesis and the socket. The wireless power transfer and the interrogation of the implanted transponders by the reader are based on the full-duplex Radiofrequency Identification standards EPC-Gen-2 so that transponders will send back the collected data through a backscattering modulation of the interrogating field [21].

As the implanted transponders do not possess an autonomous source, the establishment of a robust communication link is conditioned to the power that a small-size battery-driven UHF reader is allowed to radiate in order to overtake the power losses of the tissues and activate the implanted sensors. Such a power is moreover constrained to

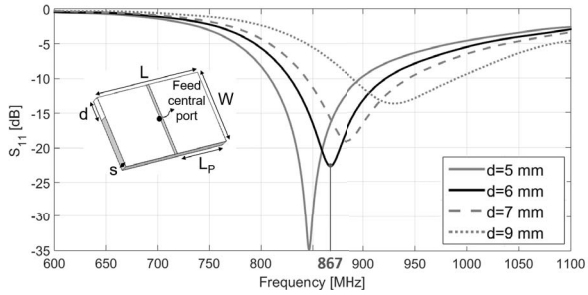

(a)

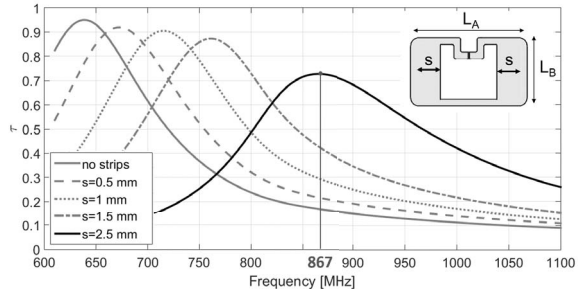

(b)

Fig. 3. Antennas involved in the evaluation of the transcutaneous telemetry system and their tuning capability: (a) Microstrip slot as interrogation antenna and its reflection coefficient ($L = 40\,mm$, $W = 25\,mm$, $L_P = 19.5\,mm$, $d = 6\,mm$ and $s = 3\,mm$) and (b) the implanted rectangular loop and its power transfer coefficient ($L_A = 12.6\,mm$, $L_B = 7.2\,mm$ and $s = 2.5\,mm$).

comply with regulation limits concerning the exposure of the human body to electromagnetic fields.

A. Arm Model

The arm stump is simulated by a realistic multi-layered cylindrical model derived from the extrusion of a cryo-sectioned forearm picture [22] (Fig. 2). The arm is inserted into a coaxial cylinder emulating the prosthetic socket, made of epoxy resin and partly leveled on top to easily allocate the slot antenna. All the electromagnetic computations to be showed next were performed by CST Microwave Studio 2017, Time-Domain Solver.

B. Interrogation Antenna and Implanted Transponder

The considered antennas are based on layouts already used in biomedical applications, such as a small loop acting as implanted tag and a microstrip slot working as interrogator. The microstrip slot is derived from a typical applicator for microwave Hyperthermia (also known as *current sheet* [23]) and later-on used for RFID sensing in [24]. The antenna (Fig. 3a) is made of two patches facing each other and shorted to the ground plane at opposite edges by means of two vertical stripes. The substrate is a 3 mm layer of Closed-cell PVC foamboard ($\varepsilon_r = 1.55$, $\sigma = 6 \cdot 10^{-4}\,S/m$). The antenna can be adjusted around 867 MHz by varying the length of the stripes (parameter d).

The rectangular loop geometry is derived from a commercial general-purpose miniaturized tag (Mecstar *Loopetto* [25]) at the purpose to simplify the experimental evaluation as

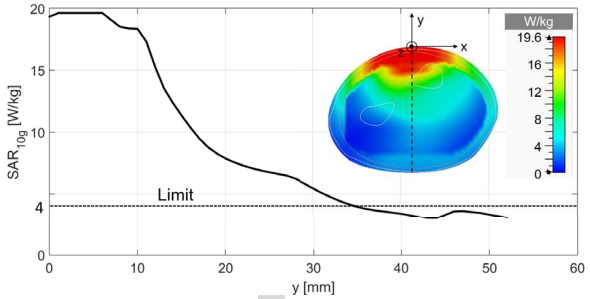

Fig. 4. Simulated SAR delivered by the microstrip slot inside the layered model of the arm's stump corresponding to $P_{av,G} = 1\,W$ and averaged onto 10 g of tissue.

described later-on. The tag is assumed to be made of an aluminum trace (thickness: $10\,\mu m$) deposited onto a PET substrate ($\varepsilon_r = 3$, $\sigma = 1.6 \cdot 10^{-2}\,S/m$, thickness: $10\,\mu m$) (Fig. 3b). The width of the smaller sides can be varied in order to tune the antenna to the chip impedance $Z_C = (12 - j120)\,\Omega$ at 867 MHz and perform some manual adjustment later on in the experimentations.

C. Specific Absorption Rate

Fig. 4 shows the computed SAR delivered by the transmitter inside the arm stump (without the implanted antenna) corresponding to a unitary input available power $P_{av,R}$ at the reader side. Values are much higher than in the case of a remote interrogating antenna as found in [14]. By considering that the safety regulation [26] requires the maximum allowed SAR in the arms, averaged onto 10 g, to be less than 4 W/kg, it follows by linearity that the maximum power emitted by the reader must be $P_{av,R} < P_{av,R}^{SAR} \simeq 23\,dBm$.

III. Link Parameterization and Constraints

The above transcutaneous link is properly modeled [27] by a two-ports network and by its self Z_{ii} and mutual Z_{ij} impedances. Port 1 and port 2 refer to the terminals of the interrogation antenna and of the implanted tag, respectively. Z_G and Z_L are the impedance of the generator connected to the reader and the RF-equivalent chip impedance. This representation accounts for possible impedance mismatch at the reader-antenna port as well as at the interconnection between the implanted antenna and the chip, caused by the disturbing effects of human body [12] and by the mutual coupling among the two antennas.

A. System Gains

Forward and backward links are parameterized [14] by means of the *Transducer Power Gain* G_T and *Round-Trip Power Gain* G_{RT}, respectively, defined [12] as:

$$G_T = \frac{P_{R\to T}}{P_{av,R}} = \frac{4R_{chip}R_G|Z_{21}|^2}{\left|(Z_{11}+Z_G)(Z_{22}+Z_{chip}) - Z_{12}Z_{21}\right|^2} \quad (1)$$

$$G_{RT} = \frac{P_{R\leftarrow T}}{P_{av,R}} = \frac{1}{4}\left|\Gamma_{in}\left(Z^{ON}\right) - \Gamma_{in}\left(Z^{OFF}\right)\right|^2 \quad (2)$$

where $\Gamma_{in}(Z_{mod}) = [Z_{in}(Z_{mod}) - Z_0]/[Z_{in}(Z_{mod}) + Z_0]$ is the reflection coefficient at the input port of the network corresponding to the two impedance states $Z_{mod} = \{Z^{ON}, Z^{OFF}\}$ of the microchip during the backscattering modulation. $Z_{in} = Z_{11} - Z_{12}Z_{21}/(Z_{22} + Z_{mod})$ is the input impedance seen by the reader toward the networks and $Z_0 = Z_G = 50\,\Omega$ is the equivalent input impedance of the reader's receiver after the circulator [14].

Hence, by assuming $Z^{ON} = Z_{chip}$ and $|Z^{OFF}| \gg |Z^{ON}|$, and introducing Z_{in} and Γ_{in} in (2) the round-trip gain can be finally expressed by simple mathematical manipulations as:

$$G_{RT} = \left|\frac{Z_G Z_{12}^2}{Z_{11} + Z_G}\right| \frac{1}{\left|(Z_{11} + Z_G)\big(Z_{22} + Z_{chip}\big) - Z_{12}Z_{21}\right|^2}. \quad (3)$$

B. Bit Error Rate

The quality of the whole link is quantified by the BER that provides an indication of the amount of lost bits during the communication between the reader and the implanted tag and hence is particularly meaningful for the measurement of physiologic signals. For an RFID link, the BER can be expressed as [28] $BER = \frac{1}{2} erfc(\frac{|V_0|m}{2\sqrt{2}\sigma})$, where $V_0 = 2\sqrt{2R_G P_{av,R}}$ is the input voltage at the reader and σ is the standard deviation of an Additive White Gaussian Noise (AWGN) corrupting the received signal. The modulation index $m = |\Gamma_{in}(Z^{ON}) - \Gamma_{in}(Z^{OFF})|/2$, can be hence derived from (2) as:

$$m = \sqrt{G_{RT}} \quad (4)$$

For the sake of the simplicity, the noise is referred to the only body plus the reader antenna at a same temperature T so that $\sigma = s\sqrt{KTR_G\Delta f}$ [29], where Δf is the frequency band of the RFID link (20 MHz at most) and K the Boltzmann constant. Then:

$$BER = \frac{1}{2} erfc\left(\frac{G_{RT}}{4}\sqrt{\frac{P_{av,R}}{KT\Delta f}}\right). \quad (5)$$

Typical UHF RFID readers require $BER < 10^{-3}$ [21] so that, by conservatively assuming $\Delta f = 20\,MHz$ and $T = 310.15\,^{\circ}K$ (human body temperature: 37°C), the minimum acceptable combination of round-trip gain and input power is (in decibel notation):

$$G_{RT} + \frac{1}{2}P_{av,R} \geq -56\,dB. \quad (6)$$

For instance, by assuming $P_{av,R} = 23\,dBm$ the minimum value of the round-trip gain that permits to establish a reliable link is $G_{RT} > -52.5\,dB$.

C. Power Margin for Reliable Links

A reliable communication link can be established by providing that the power emitted by the reader $P_{av,R}$ is simultaneously such *i*) to deliver enough power to activate the implanted microchip transponder, *ii*) to generate a backscattered signal that is strongly enough to be detected by the reader's receiver with a proper BER as in (6) and, finally, *iii*) to be compliant with SAR limits inside the body. At this purpose, the power $P_{R\rightarrow T}$ delivered by the reader to the tag's chip must exceed the chip sensitivity p_C (Forward Link). Simultaneously, the backscattered power $P_{R\leftarrow T}$ from the tag toward the reader's antenna, that is collected by the receiver, has to exceed the power sensitivity p_R of the reader (Backward Link). In formulas, it is easy to show that the available power threshold at the reader to activate the tag is (parameters expressed in dB):

$$P_{av,R} > P_{av,R}^{R\rightarrow T}|_{dB} = p_C - G_T. \quad (7)$$

The power threshold, so that reader's receiver is allowed to recognize and decode the response of the tag, is instead (parameters in dB):

$$P_{av,R} > P_{av,R}^{R\leftarrow T}|_{dB} = p_R - G_{RT}. \quad (8)$$

An additional constraint on the emitted power comes from the BER level (6), so that:

$$P_{av,R} > P_{av,R}^{BER}|_{dB} = -112\,dB - 2G_{RT}. \quad (9)$$

It is worth noticing that, in case the round trip gain is such that

$$G_{RT} < -112\,dB - p_R, \quad (10)$$

the backward link is limited by the BER constraint independently on the input power. Overall, the minimum reader power to enable both the forward and backward links and provide a reliable BER links is hence:

$$P_{av,R}^{min}|_{dB} = max\{p_C - G_T, p_R - G_{RT}, -112\,dB - 2G_{RT}\} \quad (11)$$

Finally, by denoting with $P_{av,R}^{max}$ the maximum available power the reader is capable to emit (generally 0.25-1 W), the following *constrained power margin M* of the link is introduced:

$$M(p_C, p_R, G_R, G_{RT}) = min\left\{P_{av,R}^{max}, P_{av,R}^{SAR}\right\} - P_{av,R}^{min} - P_0 \quad (12)$$

with P_0 a safe value to account for non fully controllable parameters of the system. The communication can be therefore established and reliable for a specific implanted transponder if M>0.

IV. Estimation of Read Region in the Arm and Tolerance to Misalignments

This Section investigates the two-ports gains, and accordingly the overall power margin, that can be achieved for the above described arrangement of the reader and the tag implanted as in Fig. 2, also considering some possible orientations of the tags. Then, for the most appropriate configurations, the effect of a partial misalignment between tag and reader is analyzed in order to quantify the resilience of the UHF transcutaneous link against the possible variability of the prosthesis-stump mounting.

A. Constrained Power Margin Versus the Tag Position

A first set of simulations refers to the tag placed in the position {*A, B, C*} (position *D* being equivalent to the position *B*) for possible orientations of both reader and tags as sketched in Table I. The arrows indicate a reference orientation of the two antennas with respect to the reference system in Fig. 2.

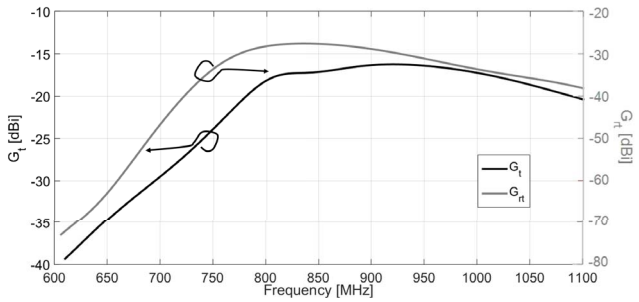

Fig. 5. Power gains of the two-ports network that parameterize the near-field reader-sensor interactions for a loop placed at position *A(x)* (just underneath the slot antenna).

TABLE I
TRANSDUCER AND ROUND-TRIP POWER GAINS (IN DB) AT 867 MHZ FOR DIFFERENT COMBINATIONS OF THE MUTUAL ORIENTATION READER-TAG

Tag	Reader (z)	Reader (x)
A (x)	**-16.9 , -30.9**	-41.9, -84.5
A (z)	-36.1, -74.7	-18.3, -36.9
B (y)	-32.4, -65.4	-44.7, -88.0
B (z)	-33.3, -68.8	-41.0, -80.2
B (-y)	**-30.5 , -61.3**	-50.6, -99.7
C (x)	**-24.1, -48.9**	-49.9, -98.5
C (z)	-47.7, -95.5	-43.0, -73.4

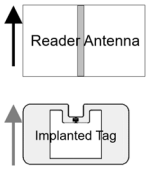

For instance, the notation *A(x)* refers to a loop placed at the position *A* and oriented so that the arrow is parallel to the *x* axis.

An example of frequency profile of the link gains is reported in Fig. 5 for tag in position *A(x)*. Both the transducer and the round-trip gains are rather stable in the whole RFID UHF band due to the intrinsic broad-banding effect of the lossy tissue of the arm model.

Results in Table I, corresponding to data at the UHF-RFID European frequency $f = 867\,MHz$, show that the most efficient mutual orientations among the interrogating slot antenna and implanted loops are such that their corresponding arrows in Table I are mutually orthogonal. In particular, a reader antenna aligned orthogonal to the arm axis (labeled as "Reader (z)") looks as the preferred arrangement.

To give some meaning to numbers of Table I, it is worth recalling that typical values of two-ports gains for implanted antennas into the limbs [14] (elbow, shoulder, hip knee) in case of an external reader (at 90cm from the skin) are $\{G_T, G_{RT}\} \simeq \{-45\,dB, -90\,dB\}$, while the transducer gain for a sensor placed onto the fingertip and a wrist reader was found [12] to be $G_T \simeq -45\,dB$.

For the most efficient *A*, *B* and *C* configurations (indicated in boldface in Table I), it is hence possible to estimate from (7), (8) the threshold powers of the forward and backward links as well as the overall constrained margin in (12). For this purpose it is assumed a typical power sensitivity of the reader ($p_R = -60\,dBm$) and two sensitivities of state of the art sensor-oriented microchips $\{p_{C1} = -5\,dBm, p_{C2} = -10\,dBm\}$ as in the AMS-SL900A [30] and RFMicron Xerxes [31] or FARSENS Rocky 100 [32], respectively. Following a standard RFID interrogation, they are moreover capable to provide an output voltage that is compatible with the EMG biasing so that local battery can be avoided. Finally, the maximum power that can be emitted by an embedded reader is assumed to be $P^{max}_{av,R} = 30\,dBm$ and the safeguard margin $P_0 = 3\,dB$ from our experience. Results summarized in Table II show that the link is almost always forward-limited since $P^{R\to T}_{av,R} > \{P^{R\leftarrow T}_{av,R}, P^{BER}_{av,R}\}$ and the constrained margins are positive for the configurations *A* and *C*. The transcutaneous link is hence feasible for sensors implanted on both the agonist (*A*) and antagonist (*C*) muscles even in case of the low-sensitivity microchip ($M = 0.9$ dB in the worst case). Instead, sensor placed in *B* results always un-readable ($M = -20\,dBm$), due to BER constraint which demands for a too high input power even in case the better chip sensitivity was used. Anyway, such a sensor could be interrogated, if needed, by a second slot antenna placed at orthogonal position w.r.t. the reference one (results labeled as *B'*).

TABLE II
THRESHOLD POWERS IN [DBM] FOR THE FORWARD AND THE BACKWARD LINKS AND THE MAXIMUM BER AND CONSTRAINED POWER MARGIN [IN DB] FOR $P^{max}_{av,R} = 30\,dBm$ AND $P_0 = 3\,dB$

	$p_C\,[dBm]$	$P^{R\to T}_{av,R}$	$P^{R\leftarrow T}_{av,R}$	$P^{BER}_{av,R}$	$M\,[dB]$
A	-5	11.9	-29.1	-20.2	8.1
	-10	6.9			13.1
B	-5	25.5	1.3	40.6	-20.6
	-10	20.5			
C	-5	19.1	-11.1	15.8	0.9
	-10	14.1			4.2
B'	-5	15.0	-20.0	-2	5
	-10	10.0			10

It is however worth noticing the interesting result that the BER constraint always dominates the backward link as $P^{BER}_{av,R} > P^{R\leftarrow T}_{av,R}$. Moreover, for the case of the high sensitivity microchip ($p_C = -10\,dBm$) and sensor placed at the deepest distance (case *C*), the BER constraints dominate the whole link, being the bottleneck of the communication ($P^{BER}_{av,R} > P^{R\to T}_{av,R}$).

B. Tolerance to Misalignments

Fig. 6a-b show the degradation of the power margin when the slot antenna is incrementally shifted along the z direction (longitudinal misalignment) and along the azimuthal angle $\phi = 0 - 90^\circ$ (axial misalignment) on the same cross-section ($z = const$). The system looks rather robust to misalignment ($M > 0$) up to $\Delta z = 1cm\,(C) - 2.5\,cm\,(A)$, practically independently on chip sensitivity, and up to $\Delta\phi = 30^\circ(A) - 40^\circ(C)$ even in the worst cases. The effect of misalignment could be mitigated, as discussed in [33], by increasing the size of an on-body interrogating antenna at the price of a further reduction of power efficiency of the system, so that a proper trade-off must be found. As expected, the margin of the tag in position *C* is narrower than for tag in position *A*.

C. Comparison With Low-Frequency Transcutaneous Links

The achieved performance of the UHF RFID link are compared in Table III with those of some low-frequency inductive transcutaneous links that have been investigated for similar

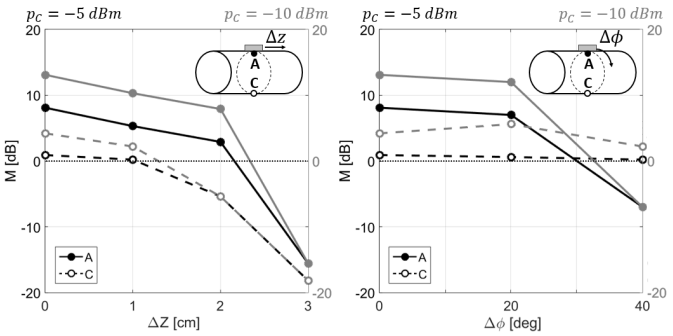

Fig. 6. Constrained power margin to establish the RFID link between the contacting slot antenna and the implanted tags at positions A (continuous lines) and C (dashed lines) for (a) longitudinal and (b) azimuthal shift of the reader's with respect to the perfectly aligned arrangement. Margin evaluated as in (12) for $P_{av,G} = 23\,dBm$, $P_0 = 3\,dB$ and the two considered chip sensitivities $p_C = -5\,dBm$ (black lines) and $p_C = -10\,dBm$ (gray lines).

TABLE III
COMPARISON AMONG PERFORMANCE OF LOW FREQUENCY AND UHF TRANSCUTANEOUS LINKS

	[6]	[8]	[35]	This work
Frequency	8 MHz	121 kHz	5 MHz	867 MHz
Size Tx [mm]	20	tailored	30	40
Size Rx [mm]	6	16	20	12.6
Depth [mm]	10	\	10	5
G_T **[dB]**	-10	\	-1.6	-17
Δz **[mm]**	\	\	25	25
$\Delta P^{min}_{av,R}(\Delta\phi = 20)$ **[dB]**[1]	0.6	0.6	0.6	1.1

applications. Since the size of the devices are not fully equivalent, such a comparison has to be therefore considered as qualitative. Overall, in spite of the much higher losses of the human tissues in the UHF band, the link performance are rather similar. The proposed architecture looks slightly more insensitive to longitudinal displacement but less efficient in the power transfer, as expected.

V. PROTOTYPES AND EXPERIMENTAL EVALUATION

To corroborate the above numerical analysis, the stump of the forearm was emulated by minced meat inserted into a real prosthetic socket. Due to the absence of lower loss tissues, like bones and fat, this configuration will provide more conservative results (lower gains) than in the previous numerical simulations.

The prototypes of both interrogating and implanted antennas are shown in Fig. 7. Tag was coated with an ultra-thin biocompatible film (Rollflex film from Master-AID, 22 μm thickness). It is worth clarifying that the considered rectangular loop tag includes the Impinj Monza R6 [34] UHF RFID microchip that does not support sensing capability as its low power threshold $p_C = -20\,dBm$ makes experimentations much easier than in case of sensor-oriented chips. The two-port gains, that are independent on the chip sensitivity, can be therefore derived even for the most challenging configurations, with the benefit

[1]As the information about the link deterioration due to angular misalignment can not be directly identified in the referenced papers, such a degradation is roughly assumed to be proportional to $|cos\Delta\phi|^2$ where $\Delta\phi$ means the angle between the normal axes of transmitting and receiving coils.

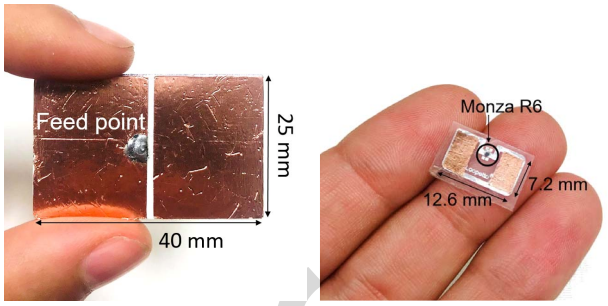

Fig. 7. Manufactured prototypes of (a) the interrogating slot antenna and (b) the loop coated by bio-compatible 22 μm polyurethane film.

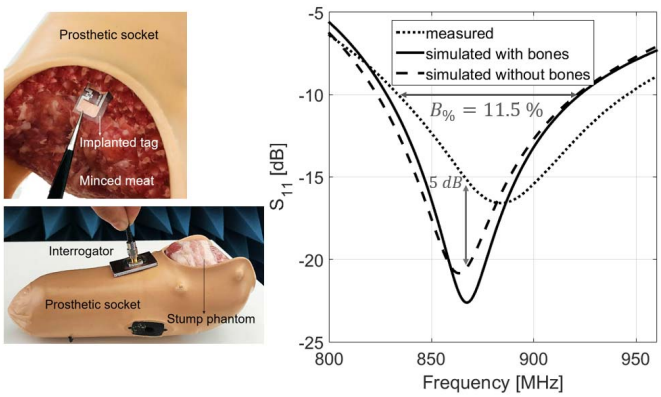

Fig. 8. (a) Experimental phantom made by minced meat filling a real prosthetic socket: Detail of the subcutaneous insertion of the tag (top) and placement of the interrogating antenna over the external surface of the prosthesis (bottom). (b) Measured reflection coefficient of the reader's antenna when it was placed over the real prosthetic socket filled with minced meat.

to can be applicable also to future generations of low-power sensing-oriented chips. The relevance of obtained results will be however discussed later on also for lower sensitivity chips.

The slot antenna was manufactured with adhesive copper and its return loss (for placement over the socket) shows that, apart for a 20 MHz shift due to the difference between the simulated ideal model and the forearm phantom (Fig. 8b), the 11.5% (at -10 dB) bandwidth looks adequate for a robust interrogation of the tag in the UHF RFID band.

A. Measurements

The tag was implanted subcutaneously, such as in Fig. 8a. The measurements setup comprised an interrogating broadband antenna connected to the Voyantic Tagformance station. The $\{A, C\}$ configurations of the previous numerical analysis were tested individually and the *activation power* $P^{min}_{av,R}$ was measured, frequency by frequency, as the minimum power emitted by the reader's generator so that the chip ID was correctly decoded by the receiver. The transducer power gain is hence computed, from (1) as $G_T = p_C/P^{min}_{av,R}$. Simultaneously, the backscattered power $P_{R\leftarrow T}$ was recorded and the round trip gain was derived from (2) as $G_{RT} = P_{R\leftarrow T}/P^{min}_{av,R}$ to make some considerations on the expected BER (that can not be directly measured with our facilities). Measurements

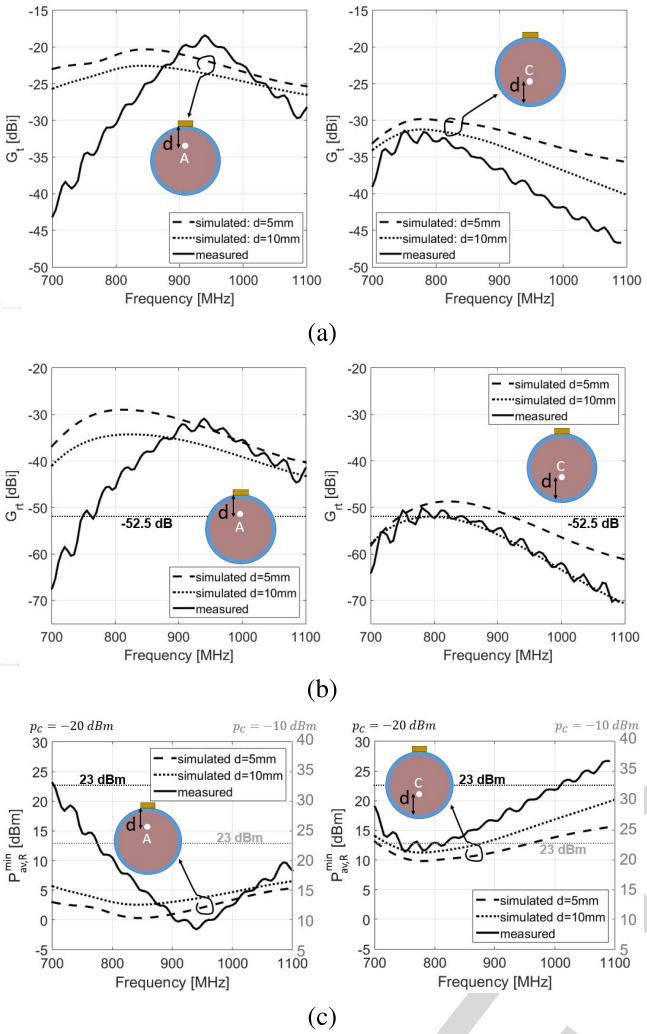

Fig. 9. Comparison among measurements and simulations for tags implanted in position A and C concerning (a) the transducer power gains and (b) the round trip gains. Horizontal lines in the G_{RT} diagrams indicate the minimum value that is compliant with $BER < 10^{-3}$ constraint for a reliable link by assuming a reader power of 23 dBm. Finally, (c) reports the extrapolated activation powers for the case of worse sensitivity sensing-oriented chips. Horizontal lines indicate the maximum power that is compliant with the SAR constraint.

are compared with the simulated results obtained from (11) of the corresponding experimental arrangements. As the true implantation depth in the experimental setup can not be accurately controlled, simulations were performed for two different implantation depths {5 mm, 10 mm}. Overall, there is a substantial coherence between measurements and simulations (Fig. 9a-b). A frequency shift of about 100 MHz between the tag in position A and position C (visible in both simulations and measurements) is due to the different coupling between tag and reader's antenna.

Focusing to the round trip gains, the comparison with the minimum value ($G_{RT} > -52.5\,dB$) that is compliant with the $BER < 10^{-3}$ constraint, shows how the interrogation of tag implanted in the position C is borderline, independently on the chip sensitivity, as it was found in simulations. Instead there is a comfortable (20 dB) margin for the tag in position A.

Starting from above two-port networks gains, the activation powers for sensor-oriented microchip ($p_C = -10\,dBm$) are

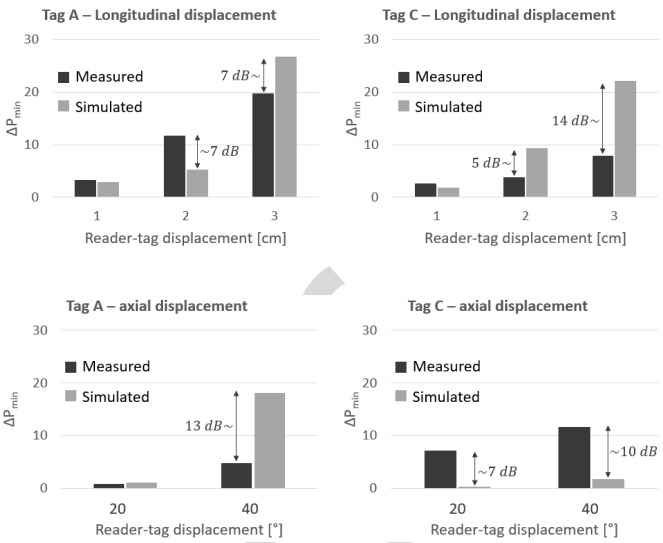

Fig. 10. Differences in the minimum activation power ΔP_{min} of the misalignments reader-tag at 867 MHz w.r.t. the links in $\{A, C\}$. Simulated values are referred to a noise band of $\Delta f = 1MHz$ as in measurements.

extrapolated in Fig. 9c and have to be compared with the maximum power (23 dBm) that is compliant with SAR limits. A sensor-tag in position A could be easily read while tag in position C would once again result in a borderline condition, at least in this simplified conservative phantom.

Finally, Fig. 10 resumes the relative minimum activation power (w.r.t. perfectly aligned configurations) vs. longitudinal and axial misalignments of the slot antenna (keeping the tag fixed). In spite of the challenge in reproducing the simulated tests in Fig. 6, the degradation of $P^{min}_{av,R}$ due to the misalignment found in the experiment follows the same trend of simulations with the full layered arm model, even if some discrepancies with measurements are visible for increasing linear and angular misalignments, especially in the most challenging configuration C probably due to the approximated knowledge of the phantom permittivity (the minced meat is dryer than the in-vivo muscle).

VI. Conclusion

Even though the compliance with the regulation on electromagnetic exposure of the human body enforces a severe limitation to the maximum power that can be emitted by the reader, the considered UHF-RFID transcutaneous telemetry allows establishing a backscattering link with a reliable $BER < 10^{-3}$. Communication can be achieved with a transponder implanted on the agonist muscle (just below the interrogating antenna) and even on the antagonist muscle in the opposite position, even if at the cost of a narrower power margin. An angular displacement up $\Delta\phi = \pm 35^\circ$ and linear displacement up to 2.5 cm with respect to the reader's axis, could be tolerated in the most convenient configuration. Moving from a low-sensitivity chip to a more performing one, the scenario is not radically changed, as the communication with tags out of the reader's axis would still return a low BER. Multiple reader's antennas could be used to enlarge the read region inside the stump. In future research, a working

prototype will be arranged to investigate the signal-level topics concerning the required sampling rate to recognize some muscular patterns and the electromagnetic susceptivity of the EMG sensor to the interrogating electromagnetic field.

REFERENCES

[1] F. Cordella *et al.*, "Literature review on needs of upper limb prosthesis users," *Front. Neurosci.*, vol. 10, p. 209, May 2016.

[2] D. Farina and R. Merletti, *Surface Electromyography: Physiology, Engineering, and Applications*, 1st ed. Piscataway, NJ, USA: Wiley, 2016.

[3] P. Morel *et al.*, "Long-term decoding of movement force and direction with a wireless myoelectric implant," *J. Neural Eng.*, vol. 13, no. 1, pp. 1–14, Feb. 2016.

[4] F. Riillo *et al.*, "Evaluating the influence of subject-related variables on EMG-based hand gesture classification," in *Proc. IEEE Int. Symp. Med. Meas. Appl.*, Lisbon, Portugal, Jun. 2014, pp. 1–5.

[5] B. D. Farnsworth, D. M. Taylor, R. J. Triolo, and D. J. Young, "Wireless implantable EMG sensing microsystem," in *Proc. 7th IEEE Sensors Conf.*, Lecce, Italy, Oct. 2008, pp. 1245–1248.

[6] B. D. Farnsworth, D. M. Taylor, R. J. Triolo, and D. J. Young, "Wireless *in vivo* EMG sensor for intelligent prosthetic control," in *Proc. Solid-State Sensors Actuators Microsyst. Conf.*, Denver, CO, USA, 2009, pp. 358–361.

[7] D. McDonnall, S. Hiatt, C. Smith, and K. S. Guillory, "Implantable multichannel wireless electromyography for prosthesis control," in *Proc. 34th Annu. Int. Conf. IEEE Eng. Med. Biol. Soc. (EMBC)*, San Diego, CA, USA, 2012, pp. 1350–1353.

[8] R. F. Weir, P. R. Troyk, G. A. DeMichele, D. A. Kerns, J. F. Schorsch, and H. Maas, "Implantable myoelectric sensors (IMESs) for intramuscular electromyogram recording," *IEEE Trans. Biomed. Eng.*, vol. 56, no. 1, pp. 159–171, Jan. 2009.

[9] G. A. DeMichele, Z. Hu, P. R. Troyk, H. Chen, and R. F. Weir, "Low-power polling mode of the next-generation IMES2 implantable wireless EMG sensor," in *Proc. 36th Annu. Int. Conf. IEEE Eng. Med. Biol. Soc. (EMBC)*, Chicago, IL, USA, 2014, pp. 3081–3084.

[10] P. F. Pasquina *et al.*, "First-in-man demonstration of a fully implanted myoelectric sensors system to control an advanced electromechanical prosthetic hand," *J. Neurosci. Methods*, vol. 244, pp. 85–93, Apr. 2015.

[11] S. Amendola, R. Lodato, S. Manzari, C. Occhiuzzi, and G. Marrocco, "RFID technology for IoT-based personal healthcare in smart spaces," *IEEE Internet Things J.*, vol. 1, no. 2, pp. 144–152, Apr. 2014.

[12] V. Di Cecco, S. Amendola, P. P. Valentini, and G. Marrocco, "Finger-augmented RFID system to restore peripheral thermal feeling," in *Proc. IEEE RFID Conf.*, Phoenix, AZ, USA, 2017, pp. 54–60.

[13] C. Occhiuzzi, G. Contri, and G. Marrocco, "Design of Implanted RFID Tags for Passive Sensing of Human Body: The STENTag," *IEEE Trans. Antennas Propag.*, vol. 60, no. 7, pp. 3146–3154, Jul. 2012.

[14] R. Lodato, V. Lopresto, R. Pinto, and G. Marrocco, "Numerical and experimental characterization of through-the-body UHF-RFID links for passive tags implanted into human limbs," *IEEE Trans. Antennas Propag.*, vol. 62, no. 10, pp. 5298–5306, Oct. 2014.

[15] E. Moradi *et al.*, "Backscattering neural tags for wireless brain-machine interface systems," *IEEE Trans. Antennas Propag.*, vol. 63, no. 2, pp. 719–726, Feb. 2015.

AQ4 [16] C. Miozzi, S. Guido, G. Saggio, E. Gruppioni, and G. Marrocco, "Feasibility of an RFID-based transcutaneous wireless communication for the control of upper-limb myoelectric prosthesis," in *Proc. 12th Eur. Conf. Antennas Propag.*, London, U.K., Apr. 2018.

[17] G. Saggio, L. Bianchi, S. Castelli, M. B. Santucci, M. Fraziano, and A. Desideri, "In vitro analysis of pyrogenicity and cytotoxicity profiles of flex sensors to be used to sense human joint postures," *Sensors*, vol. 14, no. 7, pp. 11672–11681, 2014.

[18] R. Merletti and P. Parker, *Electromyography: Physiology, Engineering, and Noninvasive Applications*. Hoboken, NJ, USA: Wiley, 2004.

[19] A. Sheibani and M. A. Pourmina, "Study and analysis of EMG signal and its application in controlling the movement of a prosthetic limb," *Health Technol.*, vol. 6, no. 4, pp. 277–284, Dec. 2016.

[20] G. Li, Y. Li, L. Yu, and Y. Geng, "Conditioning and sampling issues of EMG signals in motion recognition of multifunctional myoelectric prostheses," *Ann. Biomed. Eng.*, vol. 39, no. 6, pp. 1779–1787, Feb. 2011.

[21] D. Dobkin, *The RF in RFID*. Burlington, MA, USA: Elsevier, 2012.

[22] M. J. Ackerman, "The visible human project," *Proc. IEEE*, vol. 86, no. 3, pp. 504–511, Mar. 1998.

[23] M. K. Gospal and T. C. Cetas, "Current sheet applicators for clinical microwave hyperthermia," *IEEE Trans. Microw. Theory Techn.*, vol. 41, no. 3, pp. 431–437, Mar. 1993.

[24] S. Manzari and G. Marrocco, "Modeling and applications of a chemical-loaded UHF RFID sensing antenna with tuning capability," *IEEE Trans. Antennas Propag.*, vol. 62, no. 1, pp. 94–101, Jan. 2014.

[25] *Loopetto Mecstar Srl*. [Online]. Available: http://www.mecstar.it/it/prodotti/rfid-uhf/loopetto AQ5

[26] "Limitation of exposure of the general public to electromagnetic fields," Eur. Council, Strasbourg, France, Eur. Council Recommendation 1999/519/EC, Jul. 1999. [Online]. Available: http://ec.europa.eu/enterprise/electr_equipment/lv/rec519.pdf AQ6

[27] S. J. Orfanidis. *Electromagnetics Waves and Antennas*. [Online]. Available: http://www.ece.rutgers.edu/~orfanidi/ewa

[28] F. Fuschini, C. Piersanti, F. Paolazzi, and G. Falciasecca, "Analytical approach to the backscattering from UHF RFID transponder," *IEEE Antennas Wireless Propag. Lett.* vol. 7, pp. 33–35, 2008.

[29] R. E. Collin, *Antennas and Radiowave Propagation*. New York, NY, USA: McGraw-Hill, 1985.

[30] *Datasheet AMS-SL900A*. [Online]. Available: http://ams.com/documents/20143/36005/SL900A_DS000294_4–00.pdf

[31] *RFMicron's Xerxes*. [Online]. Available: http://rfmicron.com/rfm5000-xerxes-wireless-passive-sensor-ic/

[32] *FARSENS Rocky 100*. [Online]. Available at http://www.farsens.com/products/rocky100

[33] M. W. A. Khan, M. Rizwan, L. Sydänheimo, T. Björninen, Y. Rahmat-Samii, and L. Ukkonen, "Characterization of 3-D loop antenna to overcome the impact of small lateral misalignment in wirelessly powered intracranial pressure monitoring system," *IEEE Trans. Antennas Propag.*, vol. 65, no. 12, pp. 7405–7410, Dec. 2017.

[34] *Datasheet Monza R6*. [Online]. Available: https://support.impinj.com/hc/en-us/articles/202765328-Monza-R6-Product-Brief-Datasheet.

[35] R. Jegadeesan, S. Nag, K. Agarwal, N. V. Thakor, and Y.-X. Guo, "Enabling wireless powering and telemetry for peripheral nerve implants," *IEEE J. Biomed. Health Inform.*, vol. 19, no. 3, pp. 958–969, May 2015.

Carolina Miozzi received the M.Sc. degree in medical engineering from the University of Rome Tor Vergata in 2017, where she is currently pursuing the Ph.D. degree in electronics engineering. Her research interests include on-skin antennas and through-the-body wireless communication systems for smart health monitoring and detection of biophysical parameters. She is currently researching on the development of a wireless power transfer and transcutaneous telemetry system for the control of robotic limb prostheses, using EMG-sensors implanted subcutaneously.

Giovanni Saggio received the degree in electronics engineering and the Ph.D. degree in microelectronics and telecommunication engineering from the University of Rome Tor Vergata, Italy.

He is a Researcher and an Aggregate Professor with the University of Rome Tor Vergata, where he holds the chairs about electronics with the Engineering Faculty and the Medical Faculty. He has authored or coauthored about 200 scientific publications, eight patents, several book chapters, and is a unique author of four books about electronics. His research interests involve sensors, biotechnologies, human–machine systems, motion capture, and machine learning. He co-founded the Captiks enterprise involved in systems to measure and analyze human kinematics, the Seeti enterprise involved in virtual and augmented reality systems, and the VoiceWise enterprise involved in early diagnosis by means of voice analysis.

Emanuele Gruppioni was born in Bologna, Italy, in 1975. He received the master's degree in electronic engineering (biomedical specialization) from the University of Bologna in 2006. During the university studies, he was a Technician and the System Administrator for private companies. At the end of the studies, he obtained a scholarship in the field of organization and innovation in company management. Since 2006, he has been a Researcher for INAIL Prosthesis Centre. In 2014, he received the Degree of Certified Prosthetist and Orthotist, issued by the University of Bologna, where he has been a Professor of the course of "Orthoses and Orthopedic Aids III," Faculty of Medicine and Surgery since 2015. He is currently the Chief of Research Area with INAIL Prosthesis Centre, researching as a Project and the Technical Manager in several projects in collaboration with the Italian Institute of Technology, Genova, University "Campus Bio-Medico," Rome, Scuola Superiore Sant'Anna, Pisa, National Research Council, and Politecnico di Milano. His activities mainly concern the design and development of prosthetic limbs and new medical devices for rehabilitation. He is a Reviewer of IEEE.

Gaetano Marrocco received the Laurea degree in electronic engineering and the Ph.D. degree in applied electromagnetics from the University of L'Aquila, Italy, in 1994 and 1998, respectively.

He is a Researcher with the University of Rome Tor Vergata from 1994 to 2014, an Associate Professor of electromagnetics from 2013 to 2017, a Guest Professor with the University of Paris-est Marne la Vallèe in 2015, and has been a Full Professor with the University of Roma Tor Vergata since 2018, where he currently serves as the Director of the Medical Engineering School and the Pervasive Electromagnetics Lab. His research is mainly directed to the modeling and design of broadband and ultrawideband antennas and arrays as well as of sensor-oriented miniaturized antennas for biomedical engineering, aeronautics and radiofrequency identification (RFID). During the last decade, he carried out pioneering research on the wireless-activated sensors, and in particular, on epidermal electronics, contributing to move from the labeling of objects to the passive sensor networks in the Internet of Things era.

Prof. Marrocco is the Co-Founder and the President of the University spin-off RADIO6ENSE active in the short-range electromagnetic sensing for Industrial Internet of Things, smart manufacturing, and automotive and physical security. He serves as an Associate Editor for the IEEE JOURNAL OF RADIOFREQUENCY IDENTIFICATION. He is the Chair of the Italian Delegation URSI Commission D Electronics and Photonics. He was the Chair of the Local Committee of the V European Conference on Antennas and Propagation in 2011, the TPC Chair of the 2012 IEEE-RFID TA in Nice, France, and the TPC Track-Chair of the 2016 IEEE Antennas and Propagation International Symposium and the IEEE-RFID 2018 USA. He was a member of the IEEE Antennas and Propagation Society Awards Committee.